Proceedings of the 21st ICSMGE, Vienna, Austria, 14 – 19 June 2026. Pistrol, Adam & Schweiger (eds.)
Published by: ÖGG, Austrian Society for Geomechanics, Salzburg, Austria, ISBN 978-3-9503898-4-5
https://doi.org/10.53243/ICSMGE2026-2310

Effects of liquefaction history and partial drainage on post-liquefaction volumetric strain characteristics

Keisuke Ishikawa, Susumu Yasuda
Div. of Architectural, Civil and Environmental Engineering, Tokyo Denki University, Japan, ishikawa@g.dendai.ac.jp

Nozomu Yoshida
Institute of Science and Technology, Kanto Gakuin University, Japan

ABSTRACT: This study investigated the influence of both liquefaction history and partial drainage on the post-liquefaction volumetric strain using Toyoura sand. Liquefied soils typically undergo volumetric contraction as excess pore water pressure dissipates, a process that can affect the ground's future susceptibility to liquefaction. However, the specific effects of previous liquefaction history and the consequences of partial drainage prior to subsequent liquefaction episodes remain insufficiently understood. To address this, cyclic hollow torsional shear tests were performed under controlled laboratory conditions to analyze the volumetric strain behavior. Two experimental cases were examined: (A) the effect of liquefaction history, and (B) the effect of partial drainage before liquefaction. In Case A, specimens were subjected to multiple cycles of liquefaction and reconsolidation cycles with varying shear strain amplitudes. Results showed that the specimens with prior liquefaction history exhibited a more rapid buildup of excess pore water pressure and a notable reduction in the yield surface during reliquefaction. These specimens also exhibited similar magnitudes of volumetric strain but lower cumulative dissipated energy compared to those without a liquefaction history, suggesting that reconsolidation induces non-uniform redistribution of voids. In Case B, specimens underwent partial drainage of excess pore water pressure before liquefaction. The findings revealed that partial drainage increased the magnitude of post-liquefaction volumetric strain, indicating that pre-loading-induced alterations to the soil's void structure can significantly affect the reconsolidation characteristics. Furthermore, partially drained specimens displayed distinct shear responses, highlighting the role of loading history in shaping liquefaction behavior. These results underscore the importance of accounting for both liquefaction history and partial drainage effects when evaluating post-liquefaction ground deformation and the potential for future liquefaction under repeated seismic loading. A mechanistic understanding of these factors is essential for assessing the long-term stability of sandy soils in earthquake-prone regions.

KEYWORDS: Liquefaction history, partial drainage, volumetric strain.

1 INTRODUCTION

When subjected to a major earthquake, sandy soils are prone to liquefaction. Moreover, ground that has preciously experienced liquefaction can liquefy again during subaequent significant seismic events, as reported by Wakamatsu (2012) and Cubrinovski et al. (2011). The behavior of the ground after liquefaction can be broadly classified into three aspects: shear deformation of the soil, volumetric contraction owing to the dissipation of excess pore water pressure, and the inflow of excess pore water pressure resulting from its dissipation. Typically, liquefaction induces a rapid buildup of excess pore water pressure and the subsequent dissipation of this pressure leads to volumetric contraction, making the soil less susceptible to liquefaction.

With regards the volumetric contraction after liquefaction, Ishihara and Yoshimine (1992) experimentally demonstrated that for clean sand, the magnitude of volumetric strain increases as the relative density decreases. They also showed that the volumetric strain is positively correlated with maximum shear strain, and that the maximum volumetric strain is dependent on the soil's relative density. Unno et al. (2006) further demonstrated that when saturated and dry Toyoura sand specimens were subjected to the same shear strain histories, the resulting volumetric strains were identical. However, there is a notable gap in the literature as previous studies have not systematically investigated how a history of liquefaction affects the volumetric strain behavior of sandy soils, even when the density is held constant. Additionally, under real earthquake conditions, it is possible for a significant seismic event to generate excess pore water pressure, and for a subsequent event to occur while this excess pressure is still dissipating, potentially resulting liquefaction. Therefore, the changes in the volumetric strain characteristics of sandy soil that has undergone partial drainage before liquefaction remain unexplored.

The significance of this study is highlighted by the 2016 Kumamoto Earthquake in Japan, in which a major foreshock was followed by an even larger mainshock the next day. Some of the ground that liquefied in the foreshock liquefied again in the mainshock, while in other areas, excess pore water pressure generated during the foreshock only led to liquefaction during the mainshock as it dissipated. Understanding soil behavior under such conditions, whether through repeated liquefaction or dissipation of excess pore water pressure, is essential for understanding and accurately evaluating liquefaction resistance and post-liquefaction ground deformation.

In this study, experiments were conducted using Toyoura sand to examine the changes in volumetric strain resulting from the dissipation of excess pore water pressure after liquefaction, considering both the presence and absence of a history of liquefaction and partial drainage of excess pore water pressure.

2 EXPERIMENTAL METHOD

A cyclic hollow torsional shear test was used to conduct liquefaction behavior of Toyoura sand. The physical properties of the sand were as follows: a soil particle density (ρ_s) of 2.640 Mg/m^3 and maximum and minimum void ratios of e_{max} = 0.973 and e_{min} = 0.604, in accordance with JGS (2015). The grain-size distribution curve of Toyoura sand is presented in Figure 1.

The test specimen was a hollow, cylindrical object with an outer diameter of 100 mm, an inner diameter of 60 mm, and a height of 100 mm. The specimens were prepared using the air pluviation method, with a relative density (D_r) of 70% as the standard. After preparation, the specimens were saturated using carbon dioxide and de-aired water, followed by the application of a back pressure of 200 kN/m^2 to ensure a pore pressure coefficient (B-value) of at least 0.95. An effective confining pressure (σ'_c) of 100 kN/m^2 was applied under isotropic stress conditions, and consolidation was performed for 30 min. After

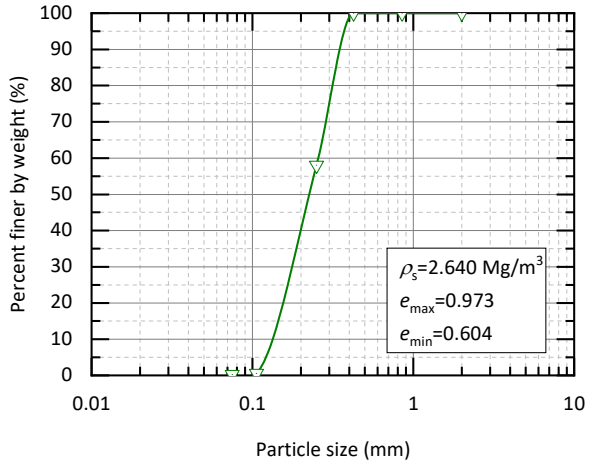

Figure 1. Grain size distribution curve.

the consolidation, cyclic shear tests were conducted under undrained conditions. Shear stress was applied in a stress-controlled manner by using a sinusoidal wave with a loading frequency of 0.05 Hz.

The volumetric change owing to the dissipation of excess pore water pressure was measured using a displacement gauge with a piston installed inside a steel cylinder. The piston movement, controlled via a screw jack, enabled integrated control of both excess pore water pressure and volumetric change.

Figure 2 illustrates the testing procedure for the presence or absence of liquefaction history (Case A). In Case A-1, the cyclic liquefaction and reconsolidation tests were repeated three times until the double-amplitude shear strain (γ_{DA}) reached 10% under a constant stress amplitude. The liquefaction test was terminated when the shear stress ratio reached zero during the cycle in which a specified double-amplitude shear strain was observed. Consequently, reliquefaction tests were performed under conditions in which residual strain was present. Case A-2 followed the same procedure as Case A-1 but with a double-amplitude shear strain of 7.5%. In Case A-3, the specimens were prepared to match the relative density after reconsolidation in Case A-1 (D_r = 79%, 82%). A liquefaction test was then conducted at a γ_{DA} of 10%. This was followed by the reconsolidation test.

Figure 3 illustrates the testing procedure for the presence or absence of the partial drainage of excess pore water pressure (Case B). In Case B-1, a cyclic liquefaction test was conducted by applying a constant shear stress amplitude until the double-amplitude shear strain reached 10%. This was followed by the reconsolidation test. In Case B-2, the excess pore water pressure was first increased to 70 kN/m^2 through pre-loading and then partially drained to 35 kN/m^2 before conducting the same experiment as in Case B-1. In Case B-3, the excess pore water pressure increased to 35 kN/m^2 before the reconsolidation test.

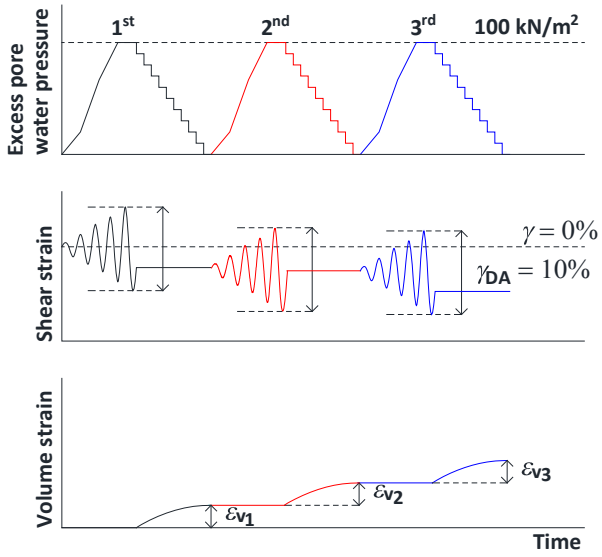

Figure 2. Case A-1: Effects of liquefaction history.

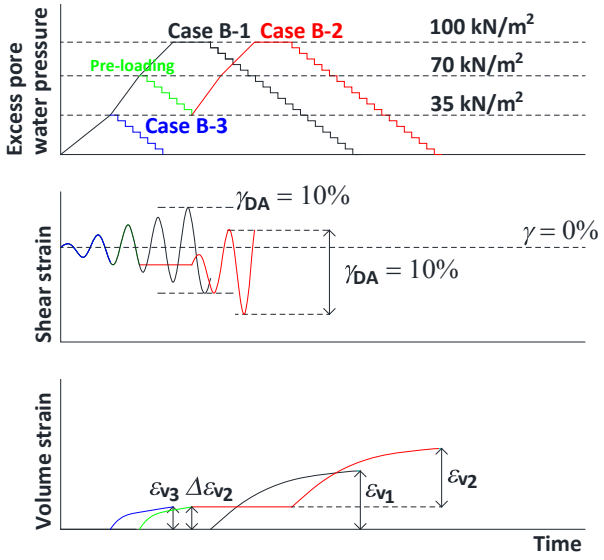

Figure 3. Case B: Effects of liquefaction after partial drainage.

3 EXPERIMENTAL RESULTS

3.1 *Effect of liquefaction history on volumetric strain*

Figure 4 presents the stress–strain relationships and effective stress paths obtained from the liquefaction test in Case A-1 (γ_{DA} = 10%).

In the first liquefaction test (black line), the excess pore water pressure increased monotonically under cyclic loading with a constant stress amplitude under all test conditions. As a result, the effective confining pressure decreased to approximately 50–40 kN/m^2, at which stage the specimens began to contract volumetrically. Upon reaching the phase transformation line, the specimen subsequently demonstrated volumetric dilation. Once the effective confining pressure was fully dissipated, the specimens experienced cyclic shear deformation until the prescribed shear strain was attained. This behavior is characteristic of medium-dense sand liquefaction. Following the first liquefaction event in Case A-1, a residual strain (γ_r) of approximately 3% persisted after the first liquefaction test, post which the shear stress returned to zero.

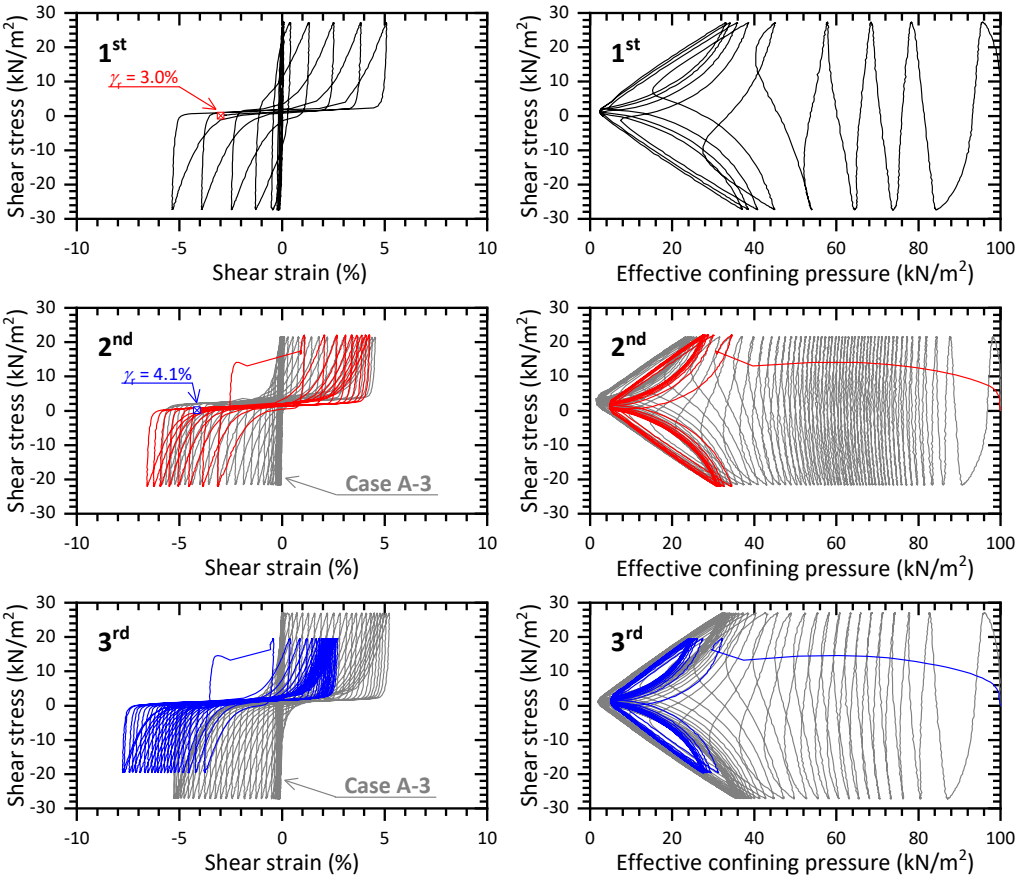

Figure 4. Case A-1: Stress-strain relationship and stress path.

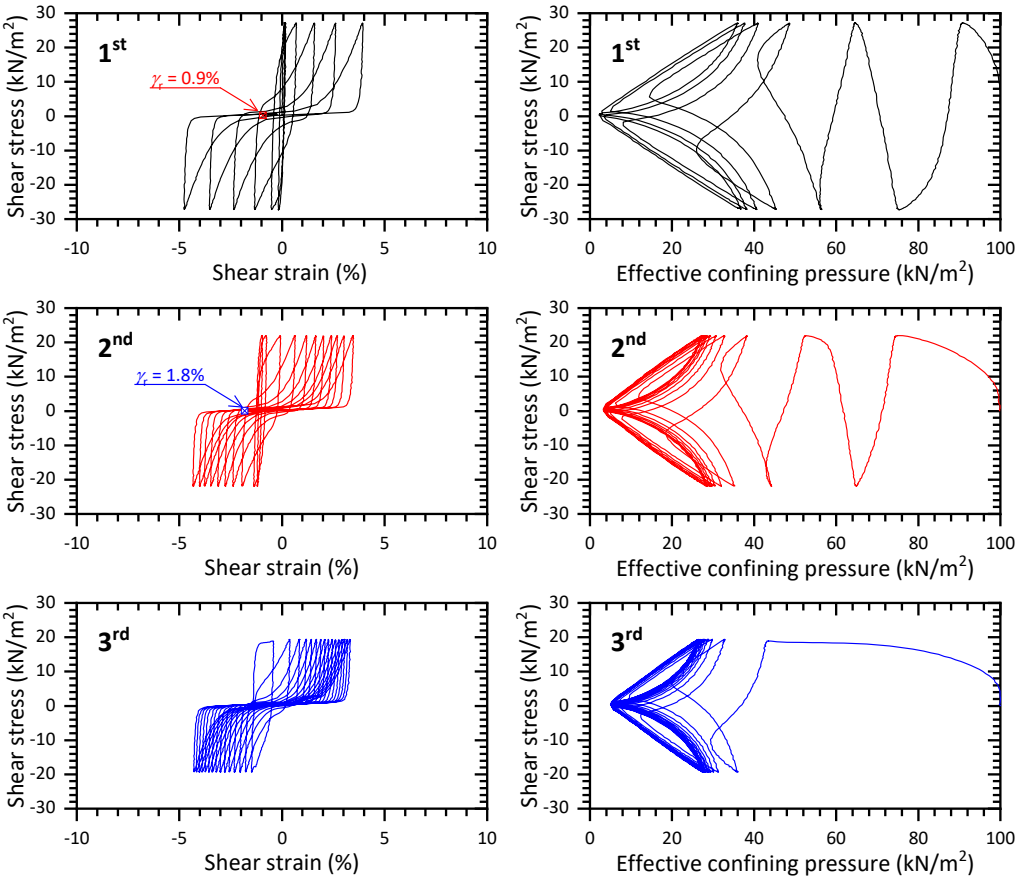

Figure 5. Case A-2: Stress-strain relationship and stress path

After reconsolidation, the second liquefaction test (red line) revealed behavioral changes influenced by the prior history of double-amplitude shear strain. Figure 4 also includes the results from Case A-3 (gray line), in which the specimen had no prior liquefaction history and was reconstituted to match the relative density after reconsolidation. In Case A-1 (γ_{DA} = 10%), the excess pore water pressure increased sharply during the first loading cycle and reached an effective confining pressure. The effective stress path also exhibited a significant reduction in the yield surface owing to the shear loading, resulting in a pronounced shear strain bias. This rapid loss of effective stress during shearing was similar to the findings of Finn et al. (1970).

Figure 5 shows the stress-strain relationship and effective stress path for Case A-2 (γ_{DA} = 7.5%). Although a lower shear stress ratio was applied compared to Case A-1, the specimen still displayed a tendency for accelerated excess pore water pressure buildup. However, its behavior differed notably from that in Case A-1. Following the second reconsolidation, the third liquefaction test (blue line) showed a response similar to that of the second liquefaction test. Notably, as the accumulated strain history increased, the shear strain bias became more pronounced.

Figure 6 illustrates the relationship between the effective confining pressure and void ratio resulting from excess pore water pressure dissipation during consolidation for each condition in Case A. In Case A-1 with γ_{DA} = 10%, the void ratio decreased significantly during reconsolidation after the first liquefaction, indicating that the specimen became denser. Furthermore, the change in the void ratio after the second liquefaction was similar to that after the first liquefaction, and despite the increased densification, the slope of the void ratio and effective confining pressure relationship remained unchanged. A similar trend was observed in Case A-3, which was adjusted to the same density after reconsolidation, where the void ratio underwent a substantial reduction during reconsolidation. However, in Case A-2, with γ_{DA} = 7.5%, the void ratio decreased significantly during reconsolidation after the first liquefaction, whereas the change in the void ratio after the second liquefaction tended to be smaller. Additionally, compared to Case A-1, the slope of the void ratio versus effective confining pressure in Case A-2 was generally smaller, reflecting a reduced sensitivity to future densification.

Figure 7 shows the relationship between the cumulative dissipated energy and volumetric strain. The cumulative dissipated energy corresponds to the area within the hysteresis loop of the stress–strain relationship. The relative densities of the specimens during liquefaction tests are shown in the figure.

After experiencing an initial liquefaction history, the volumetric strain increased with the cumulative dissipated energy, as represented by the gray dashed line in the figure. Moreover, specimens that underwent liquefaction exhibited similar levels of volumetric strain, with less dissipated energy, compared to those without a liquefaction history. These results suggest that the redistribution of voids within the specimen due to reconsolidation after the liquefaction history contributed to the observed behavior.

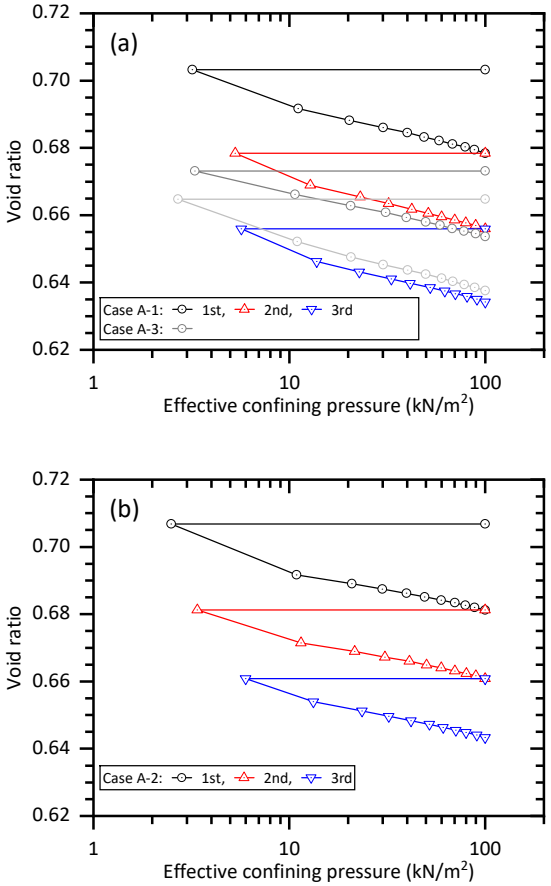

Figure 6. Relationship between the effective confining pressure and void ratio: (a) Case A-1 and Case A-3; and (b) Case A-2.

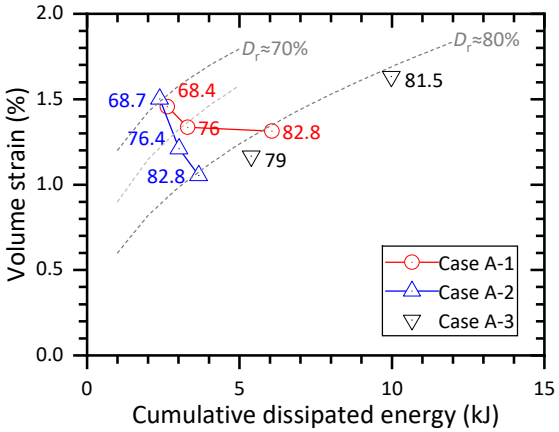

Figure 7. Cumulative dissipated energy versus volumetric strain with liquefaction history.

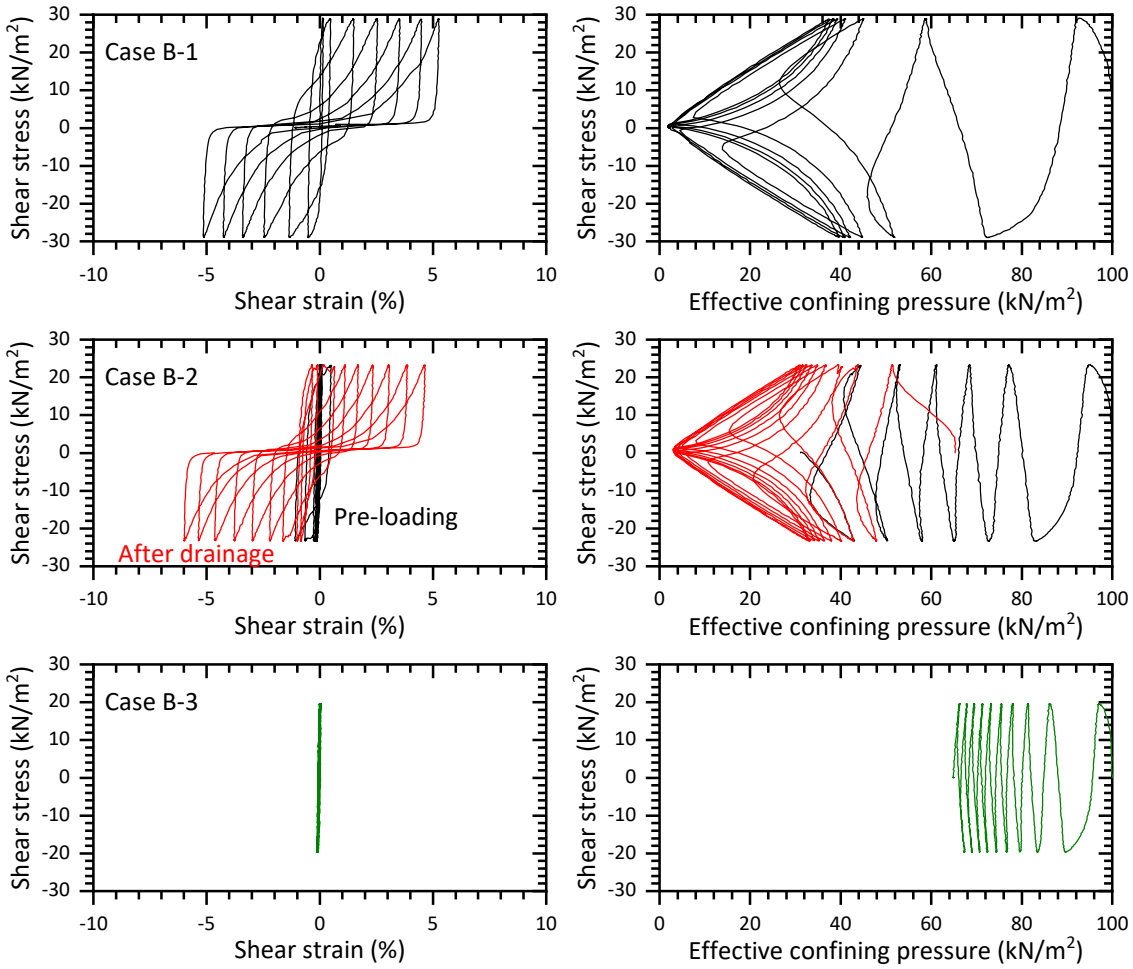

Figure 8. Stress-strain relationship and stress path with partial drainage.

3.2 *Effect of partial drainage on post-liquefaction volumetric strain*

Figure 8 shows the stress-strain relationships and effective stress paths for each condition in Case B. In Case B-1, the specimen exhibited a typical liquefaction process for medium-dense sand, where volumetric contraction occurred until the effective stress path reached the phase transformation line at approximately 50 kN/m^2. Subsequently, cyclic volumetric contraction and dilation occur, leading to a loss of effective stress and movement along the failure line trajectory until γ_{DA} = 10%. In Case B-2, during the pre-loading (black line), the cyclic shear stress loading reduced the effective confining pressure. As in Case B-1, the effective stress path reached the phase transformation line at approximately 50 kN/m^2 with γ_{DA} = 1.6% at this point. Partial drainage was applied, thereby increasing the effective confining pressure to 70 kN/m^2. The same cyclic shear stress was then reapplied (red line). During this post-drainage cyclic shearing, the effective confining pressure decreased rapidly, tracing a different path compared to the pre-loading trajectory. Once again, the phase transformation line at approximately 50 kN/m^2 was reached, after which the stress path paralleled that observed in Case B-1 until γ_{DA} = 10%. In Case B-3, as the cyclic shear loading progressed, the effective confining pressure decreased, and the excess pore water pressure reached 35 kN/m^2 when γ_{DA} = 0.17%.

Figure 9 shows the relationship between the effective confining pressure and void ratio owing to the dissipation of

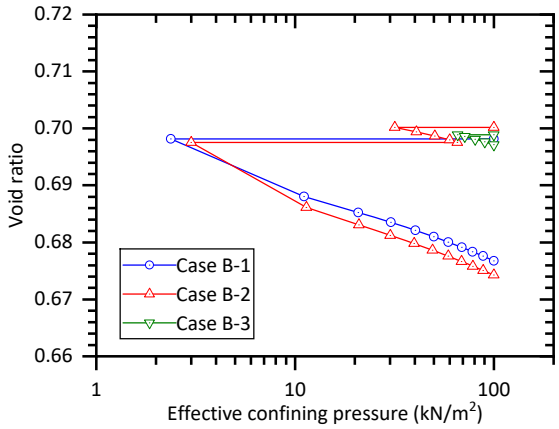

Figure 9. Relationship between the effective confining pressure and void ratio.

excess pore water pressure during the consolidation process for each condition in Case B. After applying γ_{DA} = 10% in Case B-1, the void ratio change owing to excess pore water pressure dissipation was 0.02. In contrast, in Case B-2, after partial drainage and the subsequent application of γ_{DA} = 10%, the void ratio change was 0.02, despite a slight increase in the specimen density owing to partial drainage. When comparing void ratio changes during the partial drainage process in pre-loading (σ'_c = 30–65 kN/m^2) to those in post-liquefaction consolidation in Case B-1, it is evident that the void ratio change was greater after complete liquefaction. Furthermore, in Case B-3, the void ratio change during drainage (σ'_c = 65–100 kN/m^2) was smaller than those in Cases B-1 and B-2, which had both undergone a liquefaction event.

These results indicate that the postliquefaction volumetric change in specimens subjected to partial drainage due to pre-loading was significantly larger than that in specimens without pre-loading. Moreover, these results suggest that changes in the void distribution between soil particles occurred due to the loading history and extent of the liquefaction process, thereby affecting the volumetric change characteristics during reconsolidation.

4 CONCLUSIONS

This study investigated the characteristics of volumetric strain change owing to the dissipation of excess pore water pressure after liquefaction, considering both the presence of a liquefaction history and the effect of partial drainage using Toyoura sand. The key findings are summarized as follows.

- Effect of liquefaction history: Specimens that experienced a liquefaction history exhibited a faster buildup of excess pore water pressure and a significant reduction in the yield surface during reliquefaction. Additionally, these specimens exhibited similar volumetric strains with less cumulative dissipated energy compared to specimens without a liquefaction history, suggesting a non-uniform redistribution of voids after reconsolidation.
- Effect of partial drainage: Specimens subjected to partial drainage after pre-loading exhibited different shear responses from those observed under undrained conditions. The post-liquefaction volumetric strain was greater in the specimens that underwent partial drainage, indicating that the loading history and degree of liquefaction influenced the void distribution and reconsolidation characteristics.

These findings suggest that liquefaction history and partial drainage significantly affect postliquefaction volumetric behavior, which is critical for assessing ground deformation and liquefaction resistance in repeated seismic events.

5 REFERENCES

Cubrinovski, M., Green, A. R. and Wotherspoon, L. 2011. Geotechnical reconnaissance of the 2011 Christchurch, New Zealand Earthquake. *Geotechnical Extreme Events Reconnaissance*.

Finn, W. D. L., Bransby, P. L. and Pickering, D. J. 1970. Effect of strain history on liquefaction of sand. *Journal of Soil Mechanics and Foundations Division, ASCE,* 96(SM6), 1917-1934.

Ishihara, K. and Yoshimine, M. 1992. Evaluation of settlements in sand deposits following liquefaction during earthquake. *Soils and Foundations,* 32(1), 173-188.

Japanese Geotechnical Society Standard. 2015. Test method for minimum and maximum densities of sands.

Unno, T., Kazama, M., Uzuoka, R. and Sento, N. 2006. Relation of volumetric compression of sand between under drained cyclic shear and reconsolodation after undrained cyclic shear. Journal of Japan Society of Cvil Engineering C, 6(4), 757-766.

Wakamatsu, K. 2012. Recurrent liquefaction induced by the 2011 Great East Japan Earthquake, Journal of Japan Association for Earthquake Engineering, 12(5), 69-88.